

Heavy Higgs production and decay via $e^+e^- \rightarrow Z^0 H^0 \rightarrow b\bar{b}W^+W^-$ and irreducible backgrounds at the Next Linear Collider.¹

Alessandro Ballestrero^a, Ezio Maina^a, Stefano Moretti^{a,b}

*a) Dipartimento di Fisica Teorica, Università di Torino,
and I.N.F.N., Sezione di Torino,
Via Pietro Giuria 1, 10125 Torino, Italy.*

*b) Department of Physics, University of Durham,
South Road, Durham DH1 3LE, United Kingdom.*

Abstract

The complete matrix element for $e^+e^- \rightarrow b\bar{b}W^+W^-$ has been computed at tree-level and applied to $Z^0 H^0$ production followed by $Z^0 \rightarrow b\bar{b}$ and $H^0 \rightarrow W^+W^-$, keeping into account all irreducible backgrounds, which are dominated by $t\bar{t}$ production, at the Next Linear Colliders. We find that, depending on the center of mass energies and on the search strategies, this channel can be useful for the study of the parameters of the Standard Model Higgs boson over the most part of the heavy mass range.

¹Work supported in part by Ministero dell' Università e della Ricerca Scientifica.

Introduction

The Standard Model (\mathcal{SM}) postulates the existence of a massive scalar particle, the Higgs boson H^0 , whose role is crucial in generating the spontaneous symmetry breaking of the $SU(2)_L \times U(1)_Y$ gauge group of the electroweak interactions, and in ensuring the renormalizability of the theory. Except for an upper bound of approximately 1 TeV, which can be derived from perturbative unitarity arguments [1], the model does not make any prediction on the mass M_{H^0} of such a particle.

At present, a lower limit can be extracted from LEP I ($\sqrt{s_{ee}} = M_{Z^0}$) experiments: from the results of searches for $e^+e^- \rightarrow Z^0 \rightarrow Z^{0*}H^0$ events, one derives the bound $M_{H^0} \gtrsim 60$ GeV [2].

Extensive studies have been carried out on the feasibility of discovering the Higgs particle by the next generation of high energy machines, both at pp [3, 4, 5] and at e^+e^- colliders [3, 6, 7, 8, 9, 10].

The mass region $M_{H^0} < 80 \div 90$ GeV can be studied at LEP II ($\sqrt{s_{ee}} = 160 \div 200$ GeV) whereas a Higgs with a larger mass will be searched for at pp colliders like LHC ($\sqrt{s_{pp}} = 14$ TeV) or at e^+e^- accelerators like NLC ($\sqrt{s_{ee}} = 300 \div 1000$ GeV).

At LHC the mass range $80 \text{ GeV} \lesssim M_{H^0} \lesssim 130 \text{ GeV}$ results the most difficult to study since in this case the Higgs boson mainly decays to $b\bar{b}$ pairs and the QCD background is huge. However, recent studies have shown that it is possible to detect the H^0 in the $\gamma\gamma$ decay mode [11], via the associated production with a W^\pm boson [12, 13] or a $t\bar{t}$ pair [14, 15]. For $M_{H^0} \gtrsim 130$ GeV, the Higgs can be discovered in the “gold-plated” four-lepton mode $H^0 \rightarrow Z^0 Z^0 \rightarrow \ell\bar{\ell}\ell\bar{\ell}$ [4, 5].

At NLC, with $\sqrt{s_{ee}} = 300 \div 500$ GeV, the Higgs detection can be achieved over the whole intermediate mass range $M_{Z^0} \lesssim M_{H^0} \lesssim 2M_{W^\pm}$ [16]. The two main production mechanisms are the Bjorken bremsstrahlung reaction $e^+e^- \rightarrow Z^{0*} \rightarrow Z^0 H^0$ [17] which dominates below $\sqrt{s_{ee}} = 500$ and the fusion processes $e^+e^- \rightarrow \bar{\nu}_e \nu_e W^{\pm*} W^{\mp*} (e^+e^- Z^{0*} Z^{0*}) \rightarrow \bar{\nu}_e \nu_e (e^+e^-) H^0$ [18] which dominate at larger energies. At $\sqrt{s_{ee}} \gtrsim 500$ GeV a heavy Higgs, in addition than in the 4ℓ -mode, can be detected in the four-jet modes $H^0 \rightarrow W^\pm W^\mp, Z^0 Z^0 \rightarrow jjjj$ [19, 20].

Recently, the b -tagging capabilities achieved by vertex detectors have suggested the possibility of Higgs searches through new signatures. For example, it has been shown [21] that with the b -tagging performance [22] foreseen for LHC experiments it may be possible to see the H^0 in the $t\bar{t}H^0$ production channel, with one t decaying semileptonically, followed by $H^0 \rightarrow b\bar{b}$, for $80 \text{ GeV} \lesssim M_{H^0} \lesssim 130 \text{ GeV}$, provided that

$m_t \gtrsim 130$ GeV.

It is generally expected, even in these financially troubled times for particle physics, that LHC will begin to operate approximately ten years from now, while the projects for a NLC-type of e^+e^- machine are still at a very preliminary stage. Therefore it is reasonable to assume that the Higgs, if it exists at all, will be discovered, and that its mass will be first measured, at a pp collider. However it will be impossible to study in detail all couplings between the Higgs boson and the other particles of the \mathcal{SM} at a hadron machine. For this purpose, as well as for a full analysis and a precise determination of the parameters of the top quark, a high-energy linear e^+e^- machine will be essential.

At NLC the Higgs mass can be extracted from missing mass analyses or from a direct measurement of the decay products [8]. The first method requires a measurement of the momentum of the Z^0 . This can be done easily for the e^+e^- and $\mu^+\mu^-$ decays but, with the design total luminosity of $10 fb^{-1}$, at the price of very small statistics [16]. Alternatively one can exploit the much larger $b\bar{b}$ decay mode and the capabilities of vertex detectors. We emphasize that the channel $Z^0 \rightarrow b\bar{b}$ might well be one of best ways to detect the Z^0 . In fact this mode is free from backgrounds coming from W^\pm decays, and has a branching ratio which is about five times larger than the corresponding ones to $Z^0 \rightarrow e^+e^-$ and $Z^0 \rightarrow \mu^+\mu^-$, comparable to the fraction of invisible decays $Z^0 \rightarrow \nu\bar{\nu}$ (the possibility of studying Higgs production using these latter has been examined in ref. [19]).

The missing mass method has the unique feature of being independent of assumptions on the H^0 decay modes. The $H^0 \rightarrow W^\pm W^\mp$ decays can be easily sorted out no matter how the W 's decay and the corresponding branching ratio can be directly measured. In order to obtain a precise measurement of the Higgs mass the beam energy spread resulting from bremsstrahlung and beamsstrahlung has to be taken into account. The missing mass distribution will peak at a larger value than the true Higgs mass, but this can be easily corrected for once the parameters of the machine are known. For narrow-band beam designs as DLC and TESLA [23] beamsstrahlung effects are much smaller than those of initial-state-radiation. Photon emission lowers the center-of-mass energy at which the collisions between electrons and positrons take place, decreasing the cross sections at thresholds and, on the contrary, increasing production rates at higher energies since the bulk of events are produced through s -channel annihilation and therefore scale as s^{-1} . For the mentioned designs the global effect is at most

about 20%. Since we neglect bremsstrahlung and beamsstrahlung both the number of events and their statistical significance will be slightly higher than we predict.

The direct reconstruction of the Higgs decay products requires both W 's to decay hadronically, which halves the statistics. It is however the only available mean if the Z decays to $\nu\bar{\nu}$ or for Higgs produced in fusion processes. The mass determination will suffer from the uncertainties in the measurement of jet energies but this can be somewhat improved exploiting the fact that the invariant mass of two pairs of jets must reconstruct the W mass.

In principle one could also consider the six-jet channel, $e^+e^- \rightarrow Z^0 H^0 \rightarrow Z^0 W^+ W^- \rightarrow 6j$, looking for a peak in the invariant mass distribution of pairs of vector bosons. This method however suffer from a large combinatorial background. For each event three different pairs can be formed since it is unlikely that the Z can be distinguished from the W 's, solely on the basis of their mass, when all three decay hadronically, the mass difference being comparable to the expected resolution.

Using the full matrix element for the process $e^+e^- \rightarrow b\bar{b}W^+W^-$ we are able to study the production of a heavy \mathcal{SM} Higgs (i.e., $M_{H^0} \geq 2M_{W^\pm}$) through the Bjorken bremsstrahlung reaction $e^+e^- \rightarrow Z^0 H^0$, followed by the decays $Z^0 \rightarrow b\bar{b}$ and $H^0 \rightarrow W^+W^-$, and of all irreducible backgrounds. The main background is due to $t\bar{t} \rightarrow b\bar{b}W^+W^-$ production and decay which has a much larger cross section than $e^+e^- \rightarrow Z^0 H^0$ [24, 25]. Therefore it is essential in order to assess the observability of the latter to have a complete description of the former and of the interference between the two.

The plan of the paper is as follows. In section II we give details on the calculation, while in section III we present and discuss the results. Finally, section IV is devoted to the conclusions.

Calculation

We have computed the matrix element of the process $e^+e^- \rightarrow b\bar{b}W^+W^-$ using the method of ref. [26]. As a check, we have performed the calculation also by means of the formalism [27], and compared the corresponding FORTRAN codes. The $b(\bar{b})$ quark has been treated as a massive stable particle, while the widths of all virtual $t(\bar{t})$ quark, W^\pm , Z^0 and H^0 bosons have been included in our calculations. For the top and the Higgs width we have adopted their tree-level expressions, while we have not included the effects of the width of the final state W 's [28]. For further details on the calculations, we refer to ref. [29].

The matrix element squared has to be integrated with some care in order to control the interplay among the various peaks which appear in correspondence to the possible resonances. We have divided the full set of Feynman diagrams, which are shown in fig.1, in eight subset, according to the different resonant structures, as follows:

$$t\bar{t} \rightarrow (bW^+)(\bar{b}W^-) \quad \text{diagram \# 2,} \quad (1)$$

$$t \rightarrow bW^+ \quad \text{diagrams \# 1, 7, 17,} \quad (2)$$

$$\bar{t} \rightarrow \bar{b}W^- \quad \text{diagrams \# 3, 8, 16,} \quad (3)$$

$$Z^0 H^0 \rightarrow (b\bar{b})(W^+W^-) \quad \text{diagram \# 26,} \quad (4)$$

$$Z^0 \rightarrow b\bar{b} \quad \text{diagrams \# 4, 5, 6, 11 \div 15, 18, 19,} \quad (5)$$

$$H^0 \rightarrow W^+W^- \quad \text{diagrams \# 20, 21,} \quad (6)$$

$$H^0 \rightarrow b\bar{b} \quad \text{diagrams \# 22 \div 25, 27.} \quad (7)$$

Diagrams # 9,10 and diagrams 4,6,11÷15,18,19 with an intermediate photon constitute the eighth (non-resonant) channel. If we indicate by M_i the sum of the diagrams in the i -th channel, one has

$$M_{tot} = \sum_{i=1}^8 M_i, \quad (8)$$

where M_{tot} is the total Feynman amplitude. In squaring equation (8) we take the combinations

$$\mathcal{T}_1 = |M_1|^2, \quad (9)$$

$$\mathcal{T}_2 = |M_2|^2 + 2Re[M_1M_2^*], \quad (10)$$

$$\mathcal{T}_3 = |M_3|^2 + 2Re[M_1M_3^*], \quad (11)$$

$$\mathcal{T}_4 = |M_4|^2, \quad (12)$$

$$\mathcal{T}_5 = |M_5|^2 + 2Re[M_4M_5^*], \quad (13)$$

$$\mathcal{T}_6 = |M_6|^2 + 2Re[M_4M_6^*], \quad (14)$$

$$\mathcal{T}_7 = |M_7|^2, \quad (15)$$

$$\mathcal{T}_8 = |M_8|^2 + \text{all remaining interference terms.} \quad (16)$$

Obviously

$$|M_{tot}|^2 = \sum_{i=1}^8 \mathcal{T}_i. \quad (17)$$

In the end, we have separately integrated the various contributions (9)–(16) with VEGAS [30], using $y_X = \tan^{-1} \left(\frac{Q^2 - M_X^2}{M_X \Gamma_X} \right)$ as integration variable when the X -resonance was present.

Finally, concerning the numerical part of our work, we have used the following values: $M_{Z^0} = 91.1$ GeV, $\Gamma_{Z^0} = 2.5$ GeV, $\sin^2(\theta_W) = 0.23$, $M_{W^\pm} = M_{Z^0} \cos(\theta_W) = 79.9$ GeV, $\Gamma_{W^\pm} = 2.2$ GeV, $m_b = 5.0$ GeV and $\alpha_{em} = 1/128$.

Results

If one looks at the $b\bar{b}W^+W^-$ final state in the $M_{b\bar{b}}$ versus $M_{W^+W^-}$ plane the events from the bremsstrahlung reaction will concentrate in a single blot whose size is determined by the experimental reconstruction uncertainties. On the contrary one expects the background events, mostly $t\bar{t}$ production, to fill a large region. It is however possible, for a given *top* mass, m_t , to find values of the Higgs mass for which the two double-differential distributions do no overlap. In these cases $t\bar{t}$ production can be very simply distinguished from Higgs production and detecting the H^0 is only a matter of event rate. In fig.2 the boundaries of the $d\sigma/dM_{b\bar{b}}/dM_{W^+W^-}$ distribution in the plane $(M_{b\bar{b}}, M_{W^+W^-})$ are presented for $e^+e^- \rightarrow t\bar{t}$ events for several values of m_t at $\sqrt{s} = 350$ GeV and $\sqrt{s} = 500$ GeV. It can be seen that, for $M_{b\bar{b}} = M_{Z^0}$, there is indeed a range of Higgs masses, between threshold and a maximum value which decreases with increasing m_t , for which Higgs production is effectively free of any background from $t\bar{t}$ production. For the special case $\sqrt{s} = 350$ GeV and $m_t = 170$ GeV there is also a small region at the high end of the range of Higgs masses which produce an appreciable number of events which is free from $t\bar{t}$ background.

In fig.3 and fig.4 we present the invariant mass distribution of the system recoiling against the $b\bar{b}$ pair at $\sqrt{s} = 350$ GeV and $\sqrt{s} = 500$ GeV, respectively, for $m_t = 150$ GeV and $m_t = 175$ GeV. We have required $|\cos \theta_{b\bar{b}}| < 0.8$, in order to have events which can be tagged by the microvertex detectors, and $|M_{Z^0} - M_{b\bar{b}}| < 10$ GeV. These figures have been obtained from the full matrix element. A separation of signal from background is strictly speaking impossible, however the broad structure on which the Higgs peaks rest is largely independent of M_H and one can identify it with the irreducible background. This distribution is almost flat within the range where $t\bar{t}$ production is kinematically allowed, apart from a narrow region at the boundaries where it rapidly decreases to essentially zero.

The precise composition of the total background depends on the strategy adopted

for b -tagging. If only one of the two b -jets is required to be identified there is, in addition to the irreducible background, a reducible contribution arising from the possible misidentification of a c -quark as a b -quark. If $\epsilon_{b(c)}$ is the probability for a $b(c)$ quark to satisfy a given set of tagging requirements, the probability of tagging at least one $b(c)$ of a $b\bar{b}(c\bar{c})$ pair is $P_{b(c)} = (1 - (1 - \epsilon_{b(c)})^2)$. The fraction of W decays involving a c -quark is large $B_{Wc} \equiv B(W^+ \rightarrow c\bar{s}) \approx B(W^+ \rightarrow u\bar{d}) \approx 33\%$. Therefore, the probability that a W^+W^- pair results in at least one tag is $P_{WW} = B_{Wc}^2(4\epsilon_c - \epsilon_c^2)$. Taking for example $\epsilon_b = 33\%$ and $\epsilon_c = 5\%$ [31] and defining $\sigma_0 = \sigma(e^+e^- \rightarrow ZH) \times B(H \rightarrow WW)$ the reducible background from the reaction $e^+e^- \rightarrow ZH$ is approximately equal to $\sigma_0 \times (B(Z \rightarrow udsc) \times P_{WW} + B(Z \rightarrow c) \times P_c) \approx \sigma_0 \times 2.5\%$. An additional source of fake tags are the WW pairs produced in association with a $b\bar{b}$ pair. We can estimate the corresponding cross section multiplying by $P_{WW} \approx 2\%$ the integral of the distributions in fig.3 and 4 in a 10 GeV bin centered around the Higgs nominal mass. The largest contribution is only about 0.5 fb for $\sqrt{s} = 350$ GeV, $m_t = 150$ GeV and $M_H = 185$ GeV. The sum of reducible and irreducible background is to be compared with the signal which is $\sigma_0 \times B(Z \rightarrow b) \times P_b \approx \sigma_0 \times 8\%$. An alternative option, which has the advantage of drastically reducing the irreducible background, is to impose rather loose identification requirements on both b -jets, exploiting the fact that it is less likely to mistake a cs pair for a $b\bar{b}$ pair than it is to mistake a single c -quark for a b -quark. In ref.[31] it has been shown that with vertex detectors comparable with those already in operation it is possible to achieve an efficiency for detecting $b\bar{b}$ pairs equal to .466 with an efficiency for cs pairs of .025.

Neglecting the complications due to the irreducible background for the time being, a rough estimate of the statistical significance of the signal is given by the ratio:

$$\frac{S}{\sqrt{B}} = \sqrt{P_b \mathcal{L}} \frac{\sigma(e^+e^- \rightarrow ZH \rightarrow b\bar{b}W^+W^-)}{\sqrt{\sigma(e^+e^- \rightarrow b\bar{b}W^+W^-) - \sigma(e^+e^- \rightarrow ZH \rightarrow b\bar{b}W^+W^-)}} \quad (18)$$

where \mathcal{L} is the luminosity and we integrate all cross sections, with the cuts used to produce fig.3 and 4, in a 10 GeV bin centered around the Higgs nominal mass. The ratio (18), together with the expected number of events, is presented in table I, for $\mathcal{L} = 10 \text{ fb}^{-1}$ and $\epsilon_b = 1/3$. In most cases, when the $t\bar{t}$ background is substantial, the significance is quite small and insufficient to detect the Higgs signal.

It is obvious that many features can be helpful in distinguishing signal from background events. Neglecting bremsstrahlung and beamsstrahlung effects in $t\bar{t}$ production, the energy of the two heavy quarks equals the beam energy. Moreover for each W one

can construct two invariant masses coupling the W in turn to both b 's and one of these quantities must be equal to m_t . Since the number of signal events is not too small, it is reasonable to try to increase the signal to background ratio with a more stringent set of cuts. In order to reduce as little as possible the signal we have considered events for which $|M_{Z^0} - M_{b\bar{b}}| < 10$ GeV and have required that one of the W 's, say the W^+ , failed to reproduce the kinematics of a $t\bar{t}$ final state when coupled with either of the two b 's, namely that $m_t - 10$ GeV $> |M_{W^+b(W^+\bar{b})}| > m_t + 10$ GeV and $E_{beam} - 10$ GeV $> |E_{W^+} + E_{b(\bar{b})}| > E_{beam} + 10$ GeV. The resulting cross sections, integrated over the window $|M_{H^0} - M_{W^+W^-}| < 10$ GeV, are presented in table II and III. The background has been reduced to a very small level while only between 10% and 30% of the signal has been lost and a reasonable number of events are expected over the whole range of Higgs masses we have examined. The proposed selection criteria are particularly convenient, since only one of the two W 's is required to decay hadronically, therefore about 85% of the WW decays of the Higgs are retained. This reduction factor and the b -tagging efficiency are not included in the cross section presented in table II and III.

Conclusions

We have studied, using full matrix element for the process $e^+e^- \rightarrow b\bar{b}W^+W^-$, the production of a \mathcal{SM} Higgs with $M_{H^0} \geq 2M_{W^\pm}$ through the bremsstrahlung reaction $e^+e^- \rightarrow Z^0H^0$, followed by the decays $Z^0 \rightarrow b\bar{b}$ and $H^0 \rightarrow W^+W^-$, and the corresponding irreducible background which is dominated by $t\bar{t}$ production. Selecting events containing a $b\bar{b}$ pair compatible with a decay of Z^0 , it has been shown that there are values of the Higgs and the top mass for which a simple cut on the invariant mass of the system recoiling against the $b\bar{b}$ pair is sufficient to completely eliminate the irreducible background. When the distributions $d\sigma/dM_{b\bar{b}}/dM_{W^+W^-}$ in the plane $(M_{b\bar{b}}, M_{W^+W^-})$ of signal and background events overlap, the statistical significance S/\sqrt{B} of the signal is not sufficient, in general, to unambiguously establish the presence of the Higgs with a simple missing mass analysis. Further cuts, based on the kinematics of $t\bar{t}$ production, can however drastically reduce the background while maintaining an acceptable number of events from Higgs production. Therefore we conclude that the production of a heavy \mathcal{SM} Higgs in association with a Z^0 can be observed at NLC in the decay channels $Z^0 \rightarrow b\bar{b}$ and $H^0 \rightarrow W^+W^-$.

References

- [1] M. Veltman, *Phys. Lett.* **B70** (1977) 253;
B.W. Lee, C. Quigg and G.B. Thacker, *Phys. Rev. Lett.* **38** (1977) 883; *Phys. Rev.* **D16** (1977) 1519.
- [2] ALEPH Collaboration, *Phys. Rep.* **216** (1992) 253;
DELPHI Collaboration, *Nucl. Phys.* **B373** (1992) 3;
L3 Collaboration, *Phys. Lett.* **B303** (1993) 391;
OPAL Collaboration, *Phys. Lett.* **B253** (1991) 511.
- [3] J.F. Gunion, H.E. Haber, G.L. Kane and S. Dawson, “*The Higgs Hunter Guide*”, Addison-Wesley, Reading MA, 1990.
- [4] Proceedings of the “*Large Hadron Collider Workshop*”, Aachen, 4–9 October 1990, eds. G. Jarlskog and D. Rein, Report CERN 90–10, E CFA 90–133, Geneva, 1990.
- [5] Proceedings of the “*Summer Study on High Energy Physics in the 1990s*”, ed. S. Jensen, Snowmass, Colorado, 1988;
Proceedings of the “*1990 Summer Study on High Energy Physics: Research Directions for the Decade*”, ed. E.L. Berger, Snowmass, Colorado, 1990.
- [6] Proc. of the ECFA workshop on LEP 200, A. Bohm and W. Hoogland eds., Aachen FRG, 29 Sept.–1 Oct. 1986, CERN 87-08.
- [7] Proceedings of the Workshop “*Physics and Experiments with Linear Colliders*”, Saariselkä, Finland, 9–14 September 1991, eds. R. Orawa, P. Eerola and M. Nordberg, World Scientific Publishing, Singapore, 1992.
- [8] Proc. of the Workshop “ *e^+e^- Collisions at 500 GeV. The Physics Potential*”, Munich, Annecy, Hamburg, 3–4 February 1991, ed. P.M. Zerwas, DESY pub. 92–123A/B, August 1992.
- [9] Proc. of the ECFA workshop on “ *e^+e^- Linear Colliders LC92*”, R. Settles ed., Garmisch Partenkirchen, 25 July–2 Aug. 1992, MPI-PhE/93–14, ECFA 93–154.
- [10] Proc. of the I Workshop on Japan Linear Collider (JLC), KEK 1989, KEK-Report 90–2;
Proc. of the II Workshop on Japan Linear Collider (JLC), KEK 1990, KEK-Report 91–10.

- [11] C. Seez et al., in ref.[4].
- [12] S.L. Glashow, D.V. Nanopoulos and A. Yildiz, *Phys. Rev.* **D18** (1978) 1724.
- [13] R. Kleiss, Z. Kunszt and W.J. Stirling, *Phys. Lett.* **B253** (1991) 269;
M.L. Mangano, SDC Collaboration note SSC–SDC–90–00113.
- [14] R. Raitio and W.W. Wada, *Phys. Rev.* **D19** (1979) 941;
J.N. Ng and P. Zakarauskas, *Phys. Rev.* **D29** (1984) 876.
- [15] J.F. Gunion, *Phys. Lett.* **B261** (1991) 510;
W.J. Marciano and F.E. Paige, *Phys. Rev. Lett.* **66** (1991) 2433;
A. Ballestrero and E. Maina, *Phys. Lett.* **B268** (1992) 437;
Z. Kunszt, Z. Trócsányi and W.J. Stirling, *Phys. Lett.* **B271** (1991) 247;
D.J. Summers, *Phys. Lett.* **B277** (1992) 366.
- [16] V. Barger, K. Cheung, A. Djouadi, B.A. Kniehl and P.M. Zerwas, *Phys. Rev.* **D49** (1994) 79.
- [17] J.D. Bjorken, Proceedings of the “*Summer Institute on Particle Physics*”, *SLAC Report* 198 (1976);
B.W. Lee, C. Quigg and H.B. Thacker, *Phys. Rev.* **D16** (1977) 1519;
J. Ellis, M.K. Gaillard and D.V. Nanopoulos, *Nucl. Phys.* **B106** (1976) 292;
B.L. Ioffe and V.A. Khoze, *Sov. J. Part. Nucl.* **9** (1978) 50.
- [18] D.R.T. Jones and S.T. Petkov, *Phys. Lett.* **B84** (1979) 440;
R.N. Chan and S. Dawson, *Phys. Lett.* **B136** (1984) 196;
K. Hikasa, *Phys. Lett.* **B164** (1985) 341;
G. Altarelli, B. Mele and F. Pitolli, *Nucl. Phys.* **B287** (1987) 205;
B. Kniehl, *preprint* DESY 91–128, 1991.
- [19] V. Barger, K. Cheung, B.A. Kniehl and R.J. Phillips, *Phys. Rev.* **D46** (1992) 3725.
- [20] K. Hagiwara, J. Kanzaki and H. Murayama, *Durham Univ. Report* No. DTP–91–18, 1991.
- [21] J. Dai, J.F. Gunion and R. Vega, *Phys. Rev. Lett.* **71** (1993) 2699;
J. Dai, J.F. Gunion and R. Vega, *Phys. Lett.* **B315** (1993) 355.

- [22] *Solenoidal Detector Collaboration Technical Design Report*, E.L. Berger *et al.*, Report SDC-92-201, SSCL-SR-1215, 1992.
- [23] T. Barklow, P. Chen and W. Kozanecki, in ref. [8].
- [24] W. Bernreuther, P. Igo-Kemenes, M. Jeżabek, J.H. Kühn, B. Lampe, O. Nachtmann, P. Overmann, T. Schröder, J. Steegborn, T. Teubner and P.M. Zerwas, in ref. [8].
- [25] A. Djouadi, D. Haidt, B.A. Kniehl B. Mele and P.M. Zerwas, in ref. [8].
- [26] A. Ballestrero, E. Maina, *Turin Univ. preprint* DFTT 76/93, March 1994.
- [27] K. Hagiwara and D. Zeppenfeld, *Nucl. Phys.* **B274** (1986) 1.
- [28] M. Jeżabek and J.H. Kühn, *Nucl. Phys.* **B314** (1989) 1;
C. Gao, C. Lu and W. Lu, *U. of Minnesota preprint* TPI-MINN-92/13-T, March 1992.
- [29] A. Ballestrero, E. Maina and S. Moretti, *Turin Univ. preprint* DFTT 78/93, March 1994, to be published in *Phys. Lett.* **B**.
- [30] G.P. Lepage, *Jour. Comp. Phys.* **27** (1978) 192.
- [31] H. Borner and P. Grosse-Wiesmann, in ref. [8].

Table Captions

tab.I Expected number of signal and background events and their statistical significance at $\sqrt{s} = 350$ GeV and $\sqrt{s} = 500$ GeV for a selection of Higgs masses after the cuts: $|M_{Z^0} - M_{b\bar{b}}| < 10$ GeV and $|\cos\theta_{b\bar{b}}| < 0.8$. We assume that only one b -jet is tagged with efficiency $\epsilon_b = 1/3$. The luminosity is taken to be $\mathcal{L} = 10 \text{ fb}^{-1}$.

tab.II Cross sections for $e^+e^- \rightarrow b\bar{b}W^+W^-$ at $\sqrt{s} = 350$ GeV, for five different values of M_{H^0} . The first column is the resonant contribution $e^+e^- \rightarrow Z^0H^0 \rightarrow b\bar{b}W^+W^-$ in the absence of cuts. The second and third column give the resonant cross section and the cross section obtained from all diagrams without Higgs, assuming $m_t = 150$ GeV, after the following set of cuts: $|M_{Z^0} - M_{b\bar{b}}| < 10$ GeV, $|M_{H^0} - M_{W^+W^-}| < 10$ GeV, $m_t - 10 \text{ GeV} > |M_{W^+b(W^+\bar{b})}| > m_t + 10$ GeV and $E_{beam} - 10 \text{ GeV} > |E_{W^+} + E_{b(\bar{b})}| > E_{beam} + 10$ GeV.

tab.III Cross sections for $e^+e^- \rightarrow b\bar{b}W^+W^-$ at $\sqrt{s} = 500$ GeV, for five different values of M_{H^0} . The first column is the resonant contribution $e^+e^- \rightarrow Z^0H^0 \rightarrow b\bar{b}W^+W^-$ in the absence of cuts. The second and third column give the resonant cross section and the cross section obtained from all diagrams without Higgs, assuming $m_t = 150$ GeV, after the following set of cuts: $|M_{Z^0} - M_{b\bar{b}}| < 10$ GeV, $|M_{H^0} - M_{W^+W^-}| < 10$ GeV, $m_t - 10 \text{ GeV} > |M_{W^+b(W^+\bar{b})}| > m_t + 10$ GeV and $E_{beam} - 10 \text{ GeV} > |E_{W^+} + E_{b(\bar{b})}| > E_{beam} + 10$ GeV.

Figure Captions

- fig.1** Feynman diagrams contributing in the lowest order to $e^+e^- \rightarrow b\bar{b}W^+W^-$. Internal wavy lines represent a γ , a Z^0 or a W^\pm , as appropriate. Internal dashed lines represent a Higgs boson.
- fig.2** The boundaries of the double differential distribution $d\sigma/dM_{b\bar{b}}/dM_{W^+W^-}$ in the plane $(M_{b\bar{b}}, M_{W^+W^-})$ for $e^+e^- \rightarrow t\bar{t}$ events in the narrow width approximation, at $\sqrt{s} = 350$ GeV and $\sqrt{s} = 500$ GeV, for different values of m_t , without cuts.
- fig.3** The differential distribution $d\sigma/dM_{W^+W^-}$ for $e^+e^- \rightarrow b\bar{b}W^+W^-$ (full matrix element with all Higgs contributions), at $\sqrt{s} = 350$ GeV, for $M_{H^0} = 170$ GeV (continuous line), $M_{H^0} = 185$ GeV (dashed line), $M_{H^0} = 210$ GeV (dotted line) and $M_{H^0} = 240$ GeV (chain-dashed line) with $m_t = 150$ GeV and $m_t = 175$ GeV, after the cuts: $|M_{Z^0} - M_{b\bar{b}}| < 10$ GeV and $|\cos\theta_{b\bar{b}}| < 0.8$.
- fig.4** The differential distribution $d\sigma/dM_{W^+W^-}$ for $e^+e^- \rightarrow b\bar{b}W^+W^-$ (full matrix element with all Higgs contributions), at $\sqrt{s} = 500$ GeV, for $M_{H^0} = 210$ GeV (continuous line), $M_{H^0} = 250$ GeV (dashed line) and $M_{H^0} = 300$ GeV (dotted line), with $m_t = 150$ GeV and $m_t = 175$ GeV, after the cuts: $|M_{Z^0} - M_{b\bar{b}}| < 10$ GeV and $|\cos\theta_{b\bar{b}}| < 0.8$.

M_{H^0} (GeV)	Signal	Background	S/\sqrt{B}
$\sqrt{s} = 350$ GeV $m_t = 150$ GeV			
185	40	132	3.5
210	23	80	2.6
240	10.5	71	1.3
$\sqrt{s} = 500$ GeV $m_t = 150$ GeV			
250	11.5	1.5	9.1
300	5.5	13.5	1.5
$\sqrt{s} = 500$ GeV $m_t = 175$ GeV			
250	11.5	8	4.0
300	5.5	17	1.4
$\mathcal{L} = 10$ fb ⁻¹ $\epsilon_b = 1/3$			

Table I

M_{H^0} (GeV)	σ (fb)		
	$Z^0 H^0 \rightarrow b\bar{b}W^+W^-$ no cut	$Z^0 H^0 \rightarrow b\bar{b}W^+W^-$ cut	$b\bar{b}W^+W^-$
170	13.24	10.61	1.11
180	12.07	8.74	1.35
190	8.46	5.88	1.44
200	7.05	4.99	1.48
210	5.94	4.31	1.42
$\sqrt{s} = 350$ GeV		$m_t = 150$ GeV	

Table II

M_{H^0} (GeV)	σ (fb)		
	$Z^0 H^0 \rightarrow b\bar{b}W^+W^-$ no cut	$Z^0 H^0 \rightarrow b\bar{b}W^+W^-$ cut	$b\bar{b}W^+W^-$
180	6.89	6.23	0.42
210	4.35	3.79	0.54
240	3.55	2.94	0.73
270	2.80	2.15	0.84
300	2.10	1.46	0.93
$\sqrt{s} = 500$ GeV		$m_t = 150$ GeV	

Table III

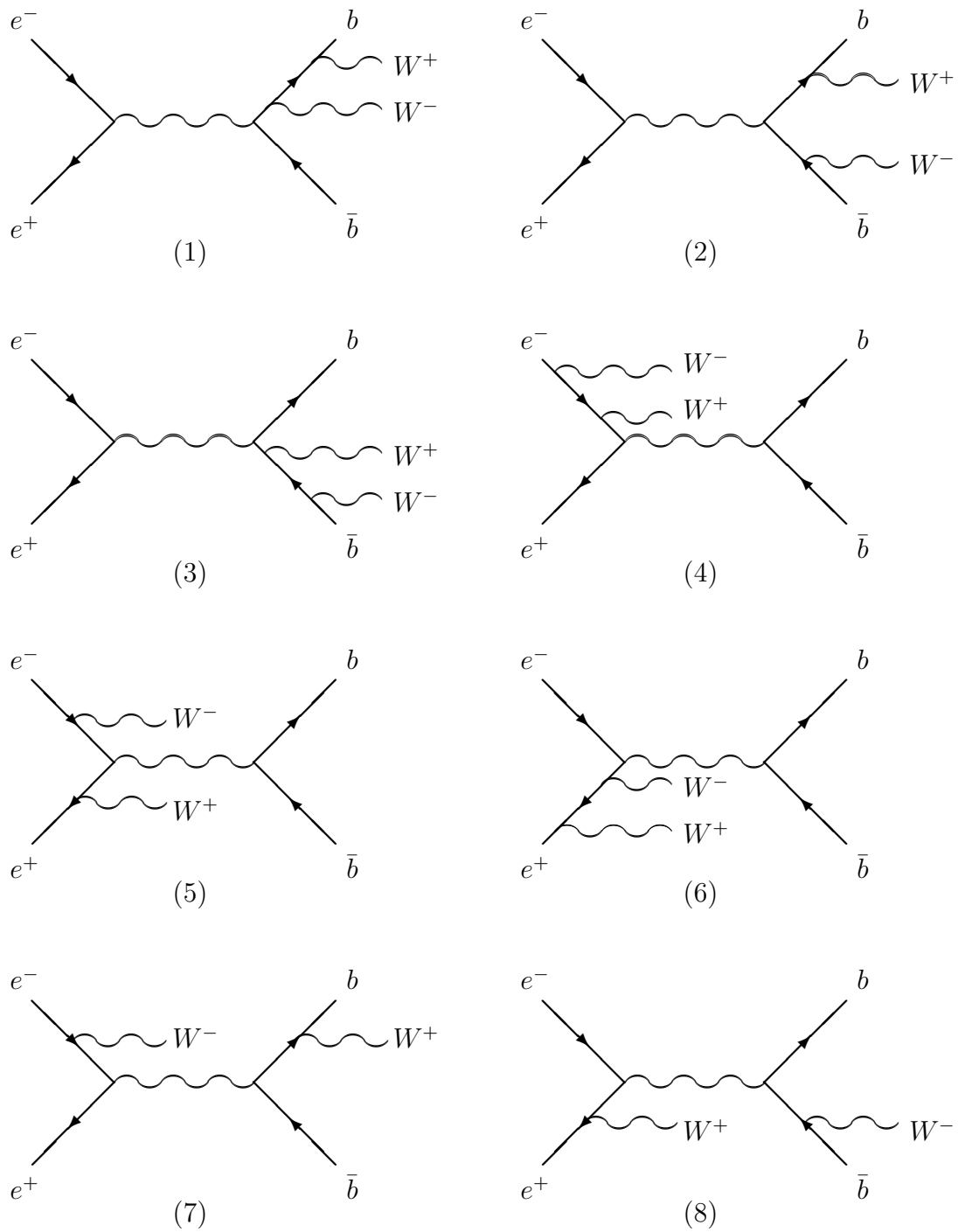


Fig. 1

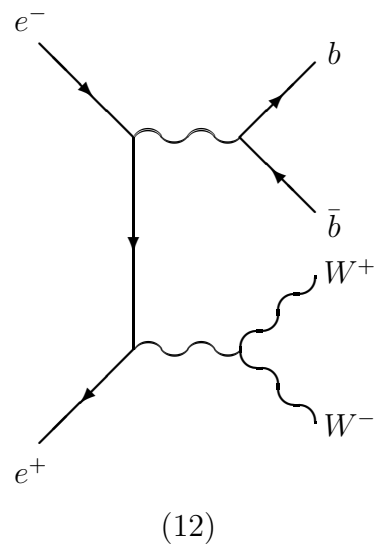
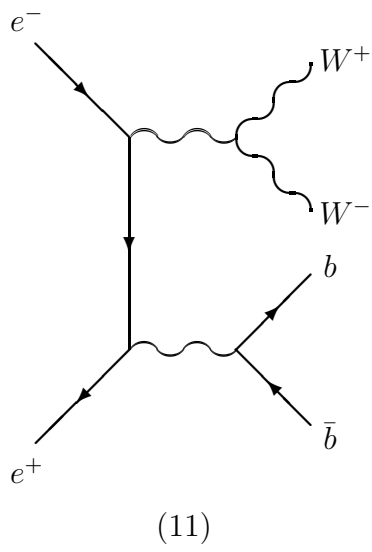
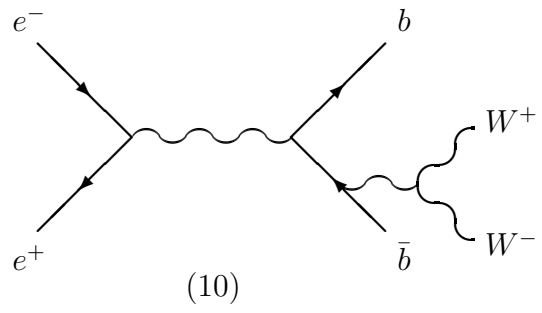
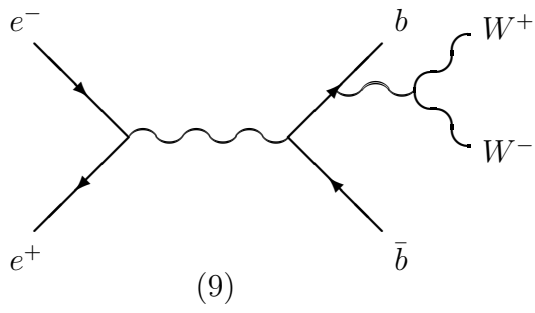


Fig. 1 (Continued)

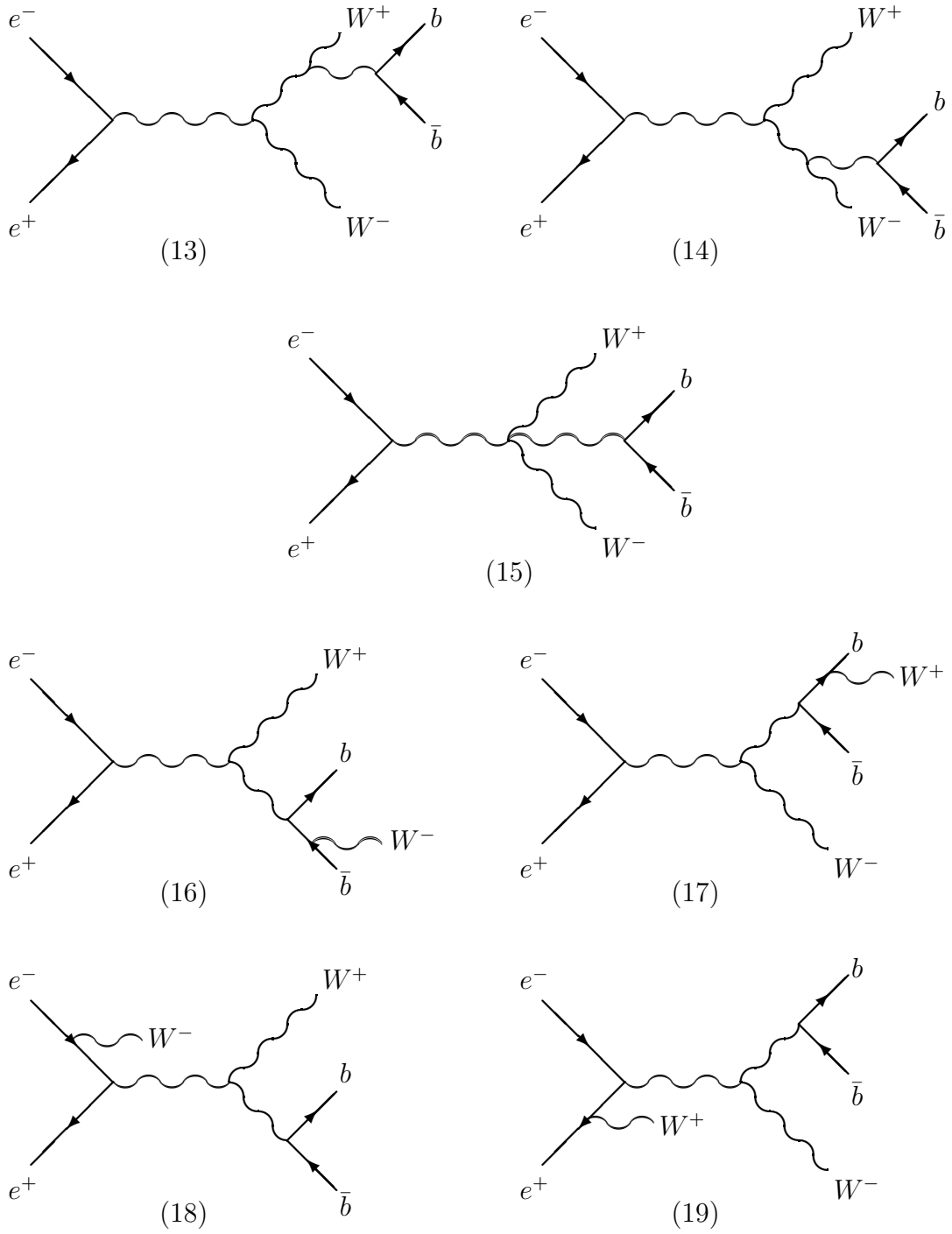


Fig. 1 (Continued)

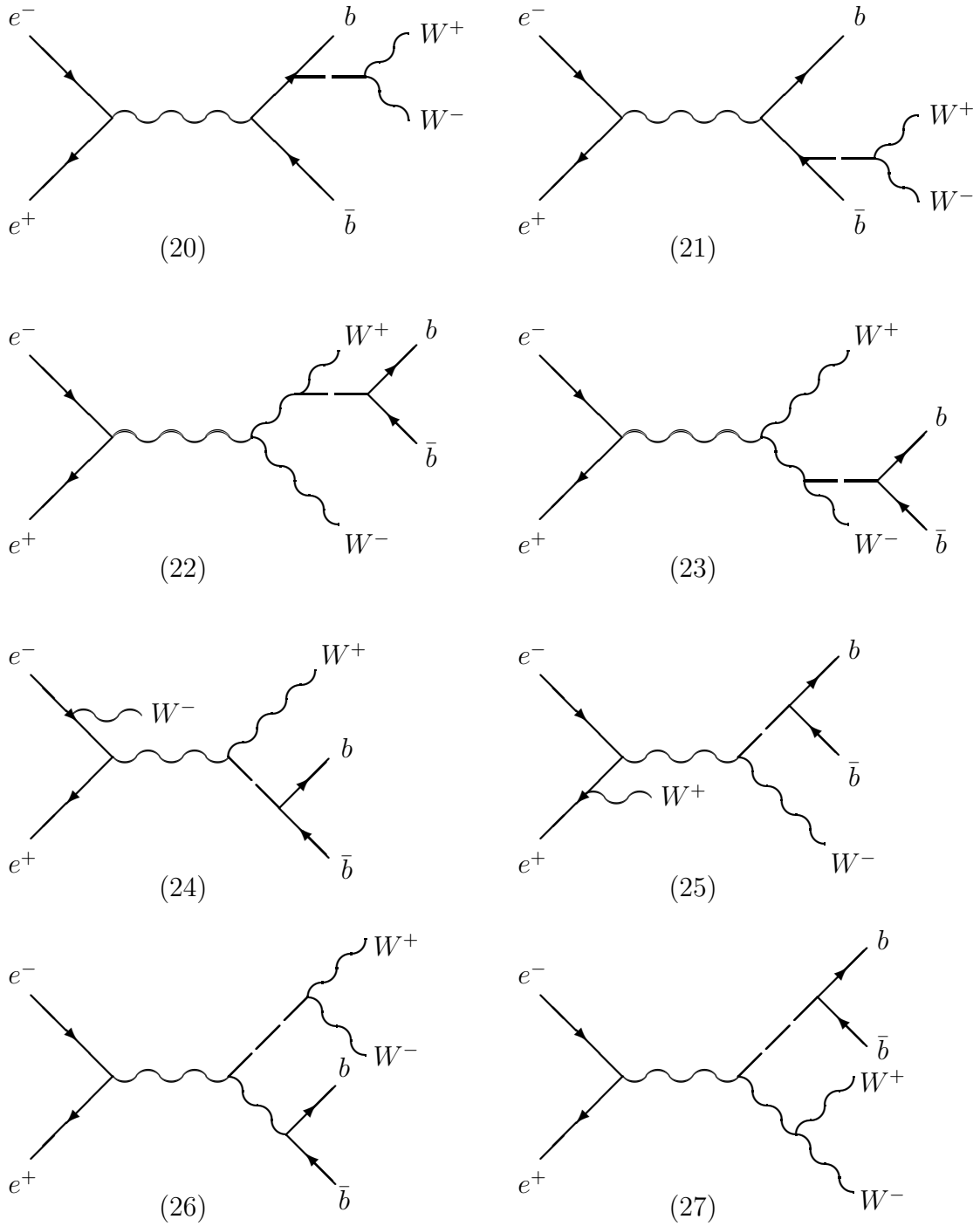


Fig. 1 (Continued)

This figure "fig1-1.png" is available in "png" format from:

<http://arxiv.org/ps/hep-ph/9409291v1>

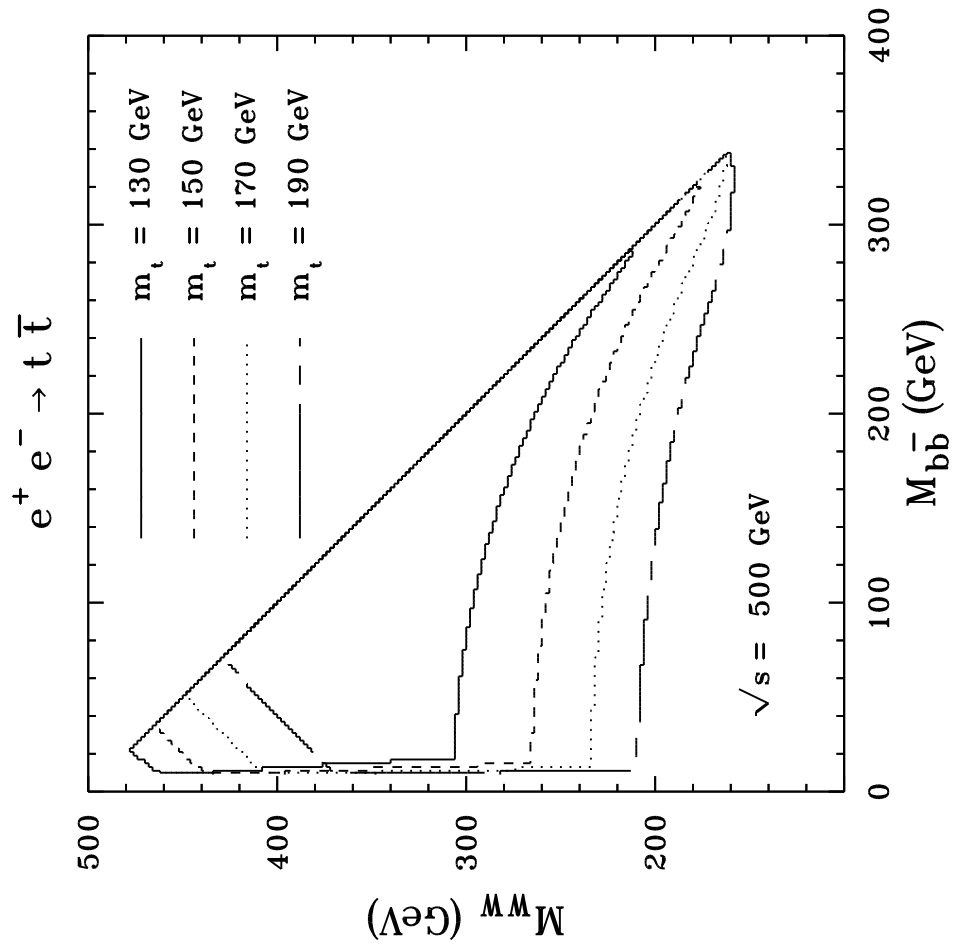
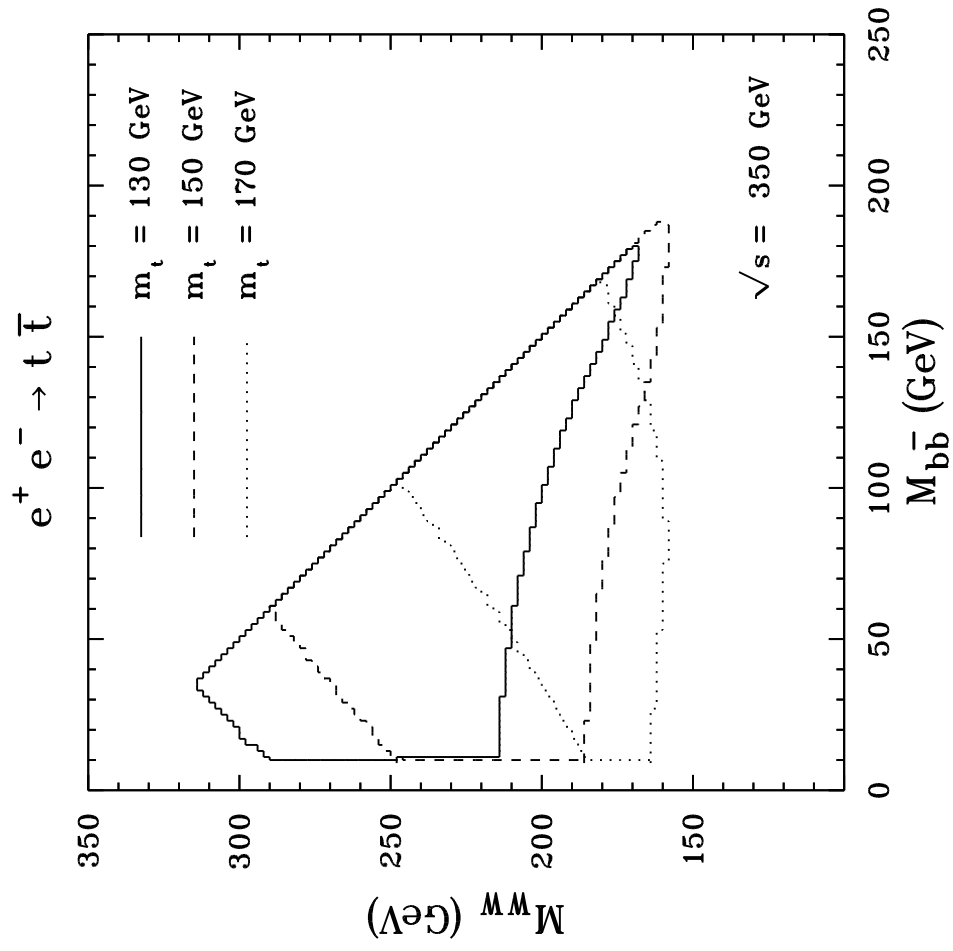


Fig. 2

This figure "fig1-2.png" is available in "png" format from:

<http://arxiv.org/ps/hep-ph/9409291v1>

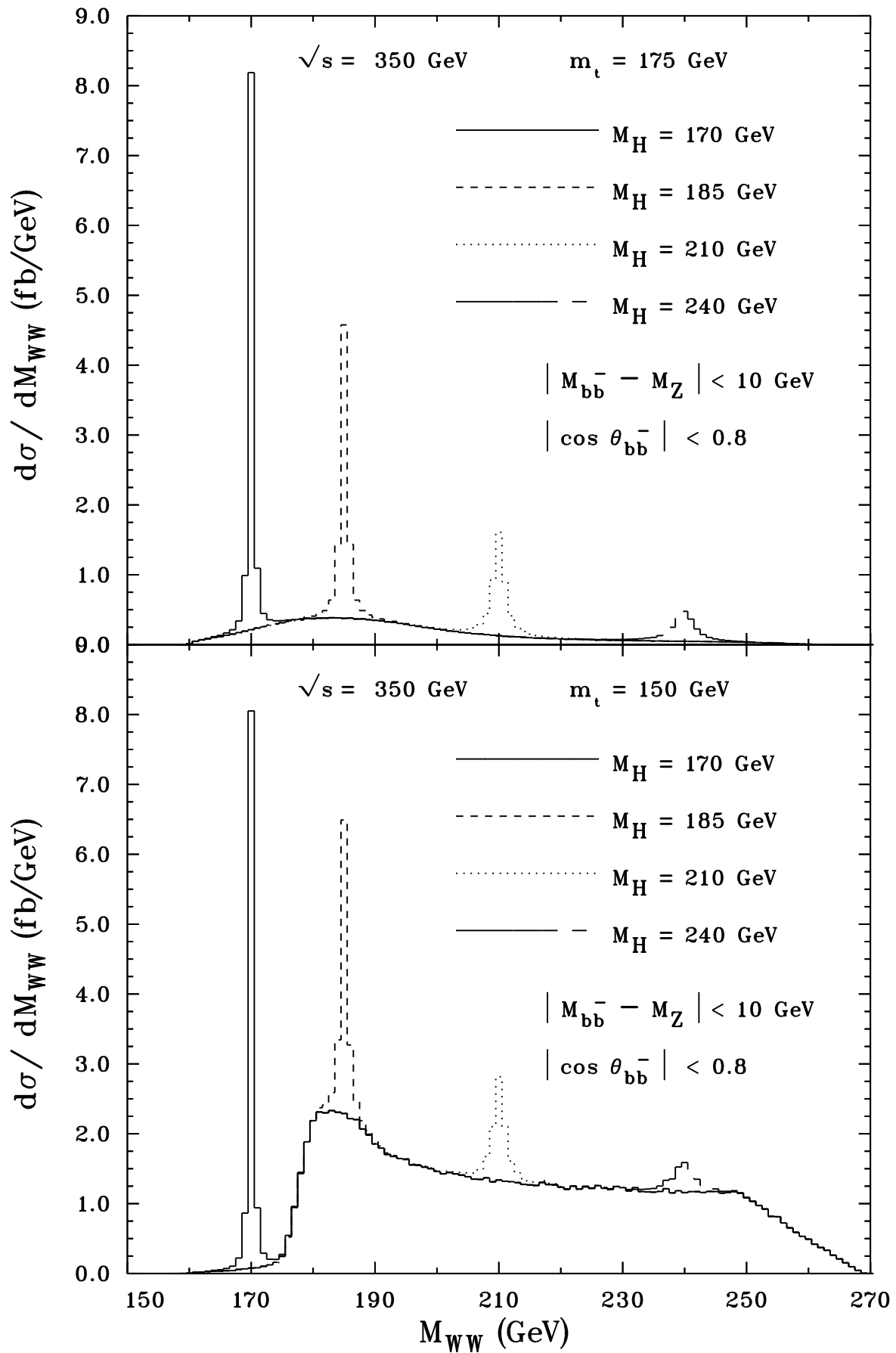
$e^+ e^- \rightarrow b\bar{b} WW$ 

Fig. 3

This figure "fig1-3.png" is available in "png" format from:

<http://arxiv.org/ps/hep-ph/9409291v1>

$$e^+ e^- \rightarrow b\bar{b} WW$$

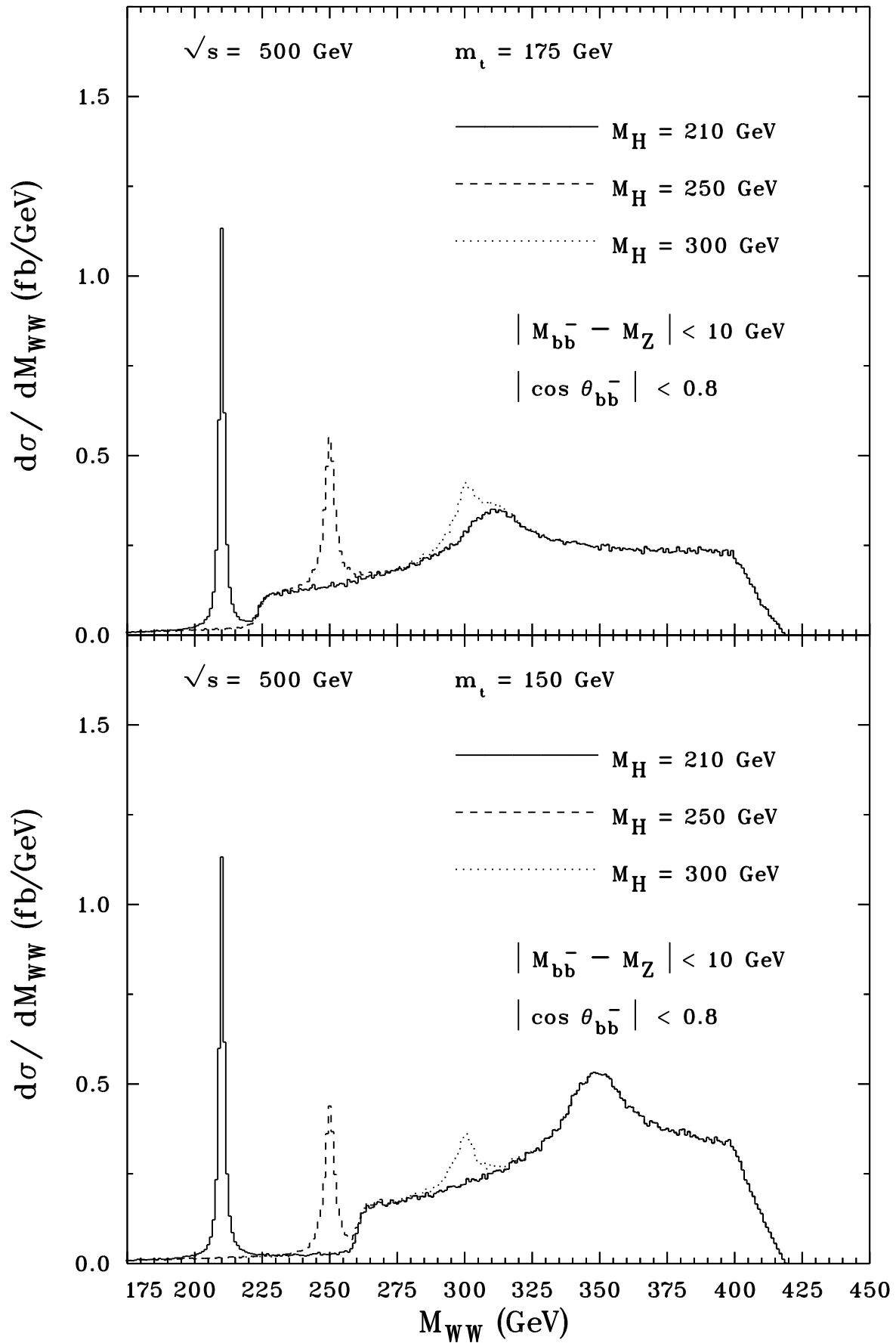


Fig. 4